DOI: 10.1021/ma9012169

Macromolecules
ARTICLE

Luminogenic Polyacetylenes and Conjugated Polyelectrolytes: Synthesis, Hybridization with Carbon Nanotubes, Aggregation-Induced Emission, Superamplification in Emission Quenching by Explosives, and Fluorescent Assay for Protein Quantitation

Wang Zhang Yuan,[†,‡] Hui Zhao,[§] Xiao Yuan Shen,[§] Faisal Mahtab,[†] Jacky W. Y. Lam,[†,‡] Jing Zhi Sun,[§] and Ben Zhong Tang*[,†,‡,§]

[†]*Department of Chemistry, Nanoscience and Nanotechnology Program, Bioengineering Graduate Program, Institute of Molecular Functional Materials, The Hong Kong University of Science & Technology (HKUST), Clear Water Bay, Kowloon, Hong Kong, China,* [‡]*HKUST Fok Ying Tung Research Institute, Nansha, Guangzhou, China, and* [§]*Department of Polymer Science and Engineering, Institute of Biomedical Macromolecules, Key Laboratory of Macromolecular Synthesis and Functionalization of the Ministry of Education of China, Zhejiang University, Hangzhou 310027, China*

Received June 7, 2009; Revised Manuscript Received November 9, 2009

ABSTRACT: Phenylacetylene and 1-pentyne derivatives containing aminated tetraphenylethene (TPE) units **1** and **2** are synthesized. The TPE-functionalized luminogens are nonemissive in dilute solutions but luminescent as solid aggregates, showing a novel behavior of aggregation-induced emission (AIE). The monomers are polymerized to their corresponding polymers **P1** and **P2** with an *E* conformation by organorhodium catalysts, although Rh-catalyzed polymerizations normally yield *Z*-rich polyacetylenes. Whereas **P1** fluoresces faintly in THF, its light emission is enhanced by aggregation in aqueous media, exhibiting an aggregation-induced emission enhancement (AIEE) effect. On the other hand, **P2** is AIE active: the emission of its nanoaggregates suspended in 90% aqueous mixture is ~57-fold stronger than that of its solution in THF. A novel superamplification effect is observed in the emission quenching of **P2** nanoaggregates by picric acid (PA): the quenching constant (K_{SV}) is nonlinearly increased with the quencher concentration and reaches a very high value in the high [PA] region ($K_{SV} \sim 350\,000\ M^{-1}$). **P1** and **P2** are transformed to conjugated polyelectrolytes $\mathbf{P1}^+$ and $\mathbf{P2}^+$ via ionization by hydrochloric acid. $\mathbf{P1}^+$ readily hybridizes with carbon nanotubes, affording functionalized $\mathbf{P1}^+$/nanotube hybrids with good water miscibility. Emission of $\mathbf{P2}^+$ in aqueous buffer is boosted when it binds to bovine serum albumin (BSA), allowing the polymer to work as a sensitive bioprobe for BSA quantitation at ultralow protein concentration (0−0.6 ppm).

Introduction

Conjugated polymers have attracted considerable interest due to their unique molecular structures, macroscopic processability, and fascinating properties,[1] which make them promising for technological applications in an array of areas, including organic light-emitting diodes,[2] photovoltaic cells,[3] field-effect transistors,[2,4] molecular wires,[5] soft lithography,[6] biomedical actuators,[7] plastic lasers,[8] optical limiters,[9] fluorescent sensors,[10] and electrochemical cells.[11] Polyacetylene is the best-known conjugated polymer, and the discovery of the metallic conductivity of its doped form has opened up a new area of research on "synthetic metals".[12] The polymer, however, is instable and intractable, which has greatly limited the scope of its practical applications. Thanks to the enthusiastic efforts of polymer chemists, various strategies have been developed to make the polymer technologically useful.[13,14] Attachment of appropriate pendant groups to the polyene backbone, for example, can help improve its processability and stability.[13] The synergistic interplay between the conjugated polyene backbone and the functional pendant groups endow the substituted polyacetylenes with new properties that are inaccessible by either the backbone and the pendant alone.[13,15] Substituted polyacetylenes carrying proper pendant groups have been found to exhibit, for example, mesomorphism,[13,15,16] luminescence,[13] permeability,[13,17] photoconductivity,[18] redox activity,[19] chain helicity,[16,20] biocompatibility,[21] and photosusceptibility.[22] It has been demonstrated that the polymers have high potentials to find practical applications in polymer light-emitting diodes,[13,23] membrane separation,[13c] fluorescence patterning,[22] rechargeable batteries,[24] nanostructured hybrids,[13,19,25] and chemosensory systems.[26]

Exploration of new functionalities and applications of substituted polyacetylenes remains to be a hot topic of current interest.[13,15a,27] Our groups have synthesized hundreds of substituted polyacetylenes that exhibit advanced materials properties[1c,13] and are endeavoring to create new polyacetylenes with singular functionalities. Recently, we have discovered an extraordinary photophysical phenomenon of aggregation-induced emission (AIE): a series of propeller-shaped molecules that are nonluminescent in the solution state are induced to emit efficiently when aggregated in poor solvents or solid state,[28] which is exactly opposite to the common aggregation-caused quenching effect of "conventional" luminophores. The AIE effect has been rationalized to be caused by the restriction to the intramolecular rotations of the luminogenic molecules by the physical restraints in the aggregate state.[28,29] The unique AIE attribute has enabled the luminogens to find high-tech applications in electroluminescence devices,[30] optically pumped lasers,[31] chemical sensors,[30,32] biological imaging,[33] etc.

*Corresponding author: Ph +852-2358-7375; Fax +852-2358-1594; e-mail tangbenz@ust.hk.

 Published on Web 11/19/2009

Chart 1. Structures of Derivatives of Phenylacetylene (1) and 1-Pentyne (2) Containing Tetraphenylethene (TPE) Unit with Aggregation-Induced Emission (AIE) Attribute

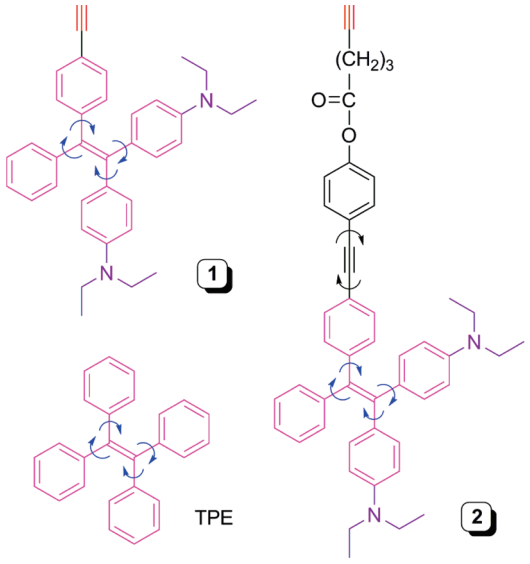

Tetraphenylethene (TPE) is a typical AIE luminogen (Chart 1).[29] It is nonemissive as an isolated molecule because its active intramolecular rotations in dilute solution effectively dissipates the energy of its exciton through nonradiative pathways. It becomes highly luminescent in the aggregate state due to the physical restriction to its intramolecular rotations in the condensed phase. Incorporation of TPE unit into polyacetylene structure may generate AIE-active conjugated polymers. The emissions of the polymer aggregates in the aqueous media may be quenched by explosives in a nonlinear fashion, as one quencher may annihilate multiple emitting species in the three-dimensional physical networks. In other words, the quenching effect may be greatly amplified with an increase in the quencher concentration. Conjugated polyelectrolytes (CPEs) are drawing increasing attention in recent years due to the unique combination of the optoelectronic activities of the conjugated polymers and the electrostatic interactions between polyelectrolytes and analytes.[34] Attachment of ionizable AIE-active pendants to polyacetylene backbone offers an alluring possibility to generate functionalized CPEs via ionization. The resultant CPEs may provide a unique platform for the fabrication of water-soluble nanohybrids[25,35] and biological sensors.[34,36] Furthermore, the AIE feature of the TPE pendants may permit the CPEs to function as probes for biomolecule detection through a "turn on" or "lighting up" mechanism.

Attracted by the prospects, in this work, we designed and synthesized phenylacetylene and 1-pentyne derivatives **1** and **2** containing aminated TPE unit (Chart 1), which is AIE-active and ionizable through amine quaternization. The acetylene monomers were polymerized by rhodium catalysts (Schemes 1 and 2), and the resultant polyacetylenes **P1** and **P2** were transformed to polyelectrolytes $\mathbf{P1}^+$ and $\mathbf{P2}^+$ via ionization of the amino pendants by hydrochloric acid (Scheme 3). The neutral and charged polymers exhibited unique functional properties when dissolved in good solvents and aggregated in poor solvents. The polymers showed superamplification effect in the emission quenching of their nanoaggregates by explosives, worked as sensitive bioprobes for protein quantitation, and acted as hybridization dispersants for dissolution of carbon nanotubes (CNTs) in aqueous media. In this paper, we report the synthesis and properties of these functionalized polyacetylenes.

Results and Discussion

Polymer Synthesis. The acetylene monomers containing the aminated TPE units were prepared by the synthetic routes shown in Schemes 1 and 2. The reactions proceeded smoothly, and the desired monomers were obtained in good yields (~61−89%). The monomers were characterized by standard spectroscopic methods, from which satisfactory analysis data were obtained (see Experimental Section for details). To transform the monomers to their polymers, organorhodium complexes $[Rh(diene)Cl]_2$ [diene = 1,5-cyclooctadiene (cod), 2,5-norbornadiene (nbd)] and $Rh^+(nbd)[C_6H_5B^-(C_6H_5)_3]$ were used as catalysts to initiate the acetylene polymerizations. The results of the polymerization reactions are summarized in Table 1.

$[Rh(diene)Cl]_2$ complexes are known as effective catalysts for polymerizations of phenylacetylene derivatives.[13] Addition of bases such as triethylamine (TEA)[13] and alkali metal amides[37] as cocatalysts normally accelerates the Rh-catalyzed acetylene polymerizations. The basic amino group in monomer **1** might serve as "cocatalyst" in the acetylene polymerization, and we thus attempted to polymerize **1** by $[Rh(diene)Cl]_2$ in the absence of a base cocatalyst. No polymeric product, however, is obtained after the mixture of **1** and $[Rh(cod)Cl]_2$ or $[Rh(nbd)Cl]_2$ has been stirred in THF for 6 h (Table 1, no. 1 or 2). The zwitterionic complex $Rh^+(nbd)[C_6H_5B^-(C_6H_5)_3]$ is known to perform well even without a cocatalyst.[38] Indeed, under similar reaction conditions (in the absence of a cocatalyst), **1** is transformed to **P1** with a high molecular weight (M_w = 26 600) in a high yield (~63%; Table 1, no. 3).

It is clear that the amino groups in **1** do not show any cocatalyst effect, and we thus added TEA as an external cocatalyst to the polymerization mixtures. The polymerization reactions in the presence of TEA proceed well to furnish polymeric products in moderate yields. Increasing the polymerization time from 6 to 24 h does not significantly affect the polymer yield but helps increase the molecular weight of the polymer obtained from the polymerization reaction catalyzed by $[Rh(nbd)Cl]_2$. In the case of $[C_6H_5B^-(C_6H_5)_3]$, both yield and molecular weight of the polymer product are increased when the polymerization time is prolonged (Table 1, no. 9). Comparison of the polymerization data reveals that $[Rh(nbd)Cl]_2$ performs better than $[Rh(cod)Cl]_2$, consistent with our previous observations.[13]

Similarly, the polymerization reaction of monomer **2** catalyzed by $[Rh(nbd)Cl]_2$ in the presence of TEA gives better result than that catalyzed by the $[Rh(cod)Cl]_2$/TEA mixture (cf. Table 1, nos. 10 and 11). $Rh^+(nbd)[C_6H_5B^-(C_6H_5)_3]$ catalyst shows the best performance: the polymerization catalyzed by the zwitterionic complex affords a polymer with a narrow molecular weight distribution (1.35) in a good yield (64.2%).

Structural Characterization. Spectroscopic techniques were employed to characterize the structures of the polymeric products. All the polymers give satisfactory analysis data corresponding to their expected structures. An example of the IR spectrum of **P1** is shown in Figure 1; the spectrum of its monomer is also given in the same figure for comparison. The monomer shows absorption bands at 3285 and 2104 cm^{-1}, which are assignable to the stretching vibrations of ≡CH and C≡C, respectively. These bands are absent in the spectrum of **P1**, indicating that the triple bond of the monomer has been fully consumed by the polymerization reaction.

Figure 2 shows the ^1H NMR spectra of monomer **1** and its polymer **P1**. The polymer gives no peak at $\delta \sim 3.0$, where

Scheme 1. Synthesis of TPE-Containing Poly(phenylacetylene) (P1)

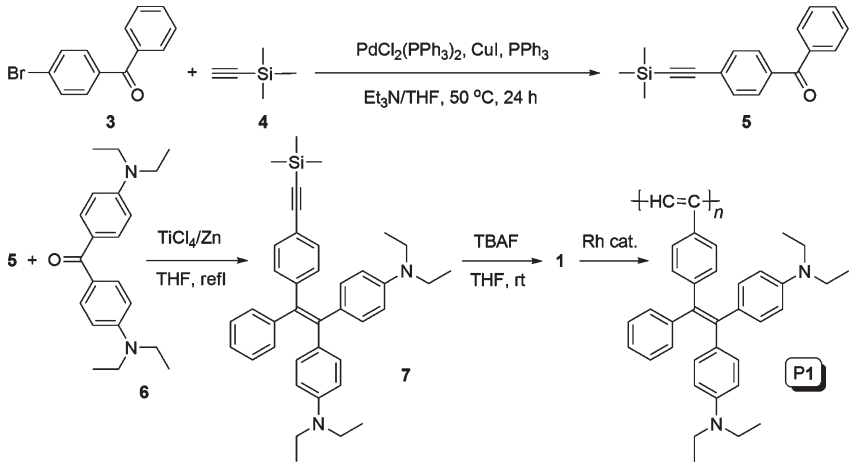

Scheme 2. Synthesis of TPE-Containing Poly(1-pentyne) (P2)

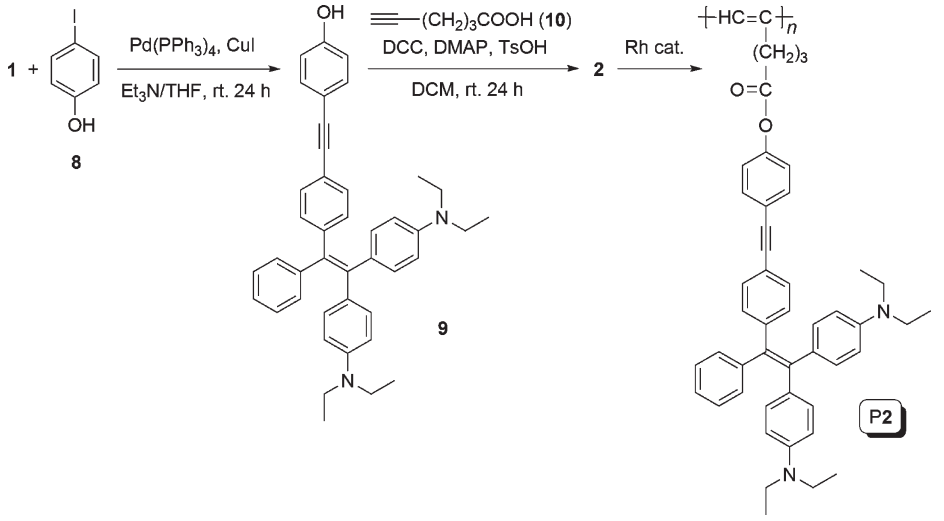

acetylene proton resonates. This indicates that the acetylenic triple bond of **1** has been transformed to the olefinic double bond by the polymerization reaction, which is consistent with the conclusion drawn from the IR spectral data. Poly(phenylacetylene) derivatives prepared from Rh-catalyzed polymerizations usually show peaks in δ 5.50−5.80, which are associated with the resonances of *Z-s-E* olefinic protons in the polyene backbone.[1c,13] No peak, however, is observed in this chemical shift region in the spectrum of **P1** (Figure 2B). It is suspected that **P1** may possess an *E-s-Z* backbone conformation, the resonance of whose olefinic proton is merged with those of the aromatic protons.[18b] To examine this assumption and to exclude the interference from the solvent signal of chloroform-*d* at $\delta \sim 7.26$, we measured the ^{1}H NMR spectrum of **P1** in deuterated dichloromethane (DCM-d_2; Supporting Information, Figure S1) and integrated the areas of the resonance peaks. As shown in Figure S2 in the Supporting Information, the ratio of the integrated areas of the resonance peaks in the different chemical shift regions is about 18:8:12, matching very well with the numbers of the protons for the aromatic and olefinic units, methylene groups, and methyl groups in **P1**. This confirms that the polyene backbone of the polymer is indeed *E-s-Z* in conformation. The ^{1}H NMR spectrum measured in dimethyl-d_6 sulfoxide (DMSO) further proves that the polymer possesses an *E-s-Z* backbone conformation (Supporting Information, Figure S3).

Figure 3 shows the ^{13}C NMR spectrum of **P1** along with that of its monomer **1**. While the acetylenic carbon atoms of monomer **1** resonate at δ 83.31 (≡C) and δ 76.01 (HC≡), these peaks are completely absent in the spectrum of **P1**. This result agrees well with those of the IR and ^{1}H NMR analyses, duly verifying the successful synthesis of **P1**. Similarly, the spectroscopic analysis data of **P2** (Supporting Information, Figures S5−S7) substantiate that **P2** has been successfully synthesized and that the polymer also possesses an unusual *E-s-Z* backbone conformation. Although the amino groups in monomers **1** and **2** do not show any cocatalyst effect (vide supra), the "abnormal" *E-s-Z* backbone conformation of their polymers **P1** and **P2** suggests that the amino groups in the monomers may have complexed with the rhodium catalyst, and the thus-formed active species may have exerted influence on the stereochemistry involved in the propagation steps of the acetylene polymerization reactions.

Stability and Absorptivity. Poly(phenylacetylene) and poly(1-alkyne) are parent forms of **P1** and **P2**, respectively. Both of the parent polymers are unstable: poly(phenylacetylene) starts to lose its weight when heated to about 200 °C under nitrogen, while the weight loss of poly(1-hexyne) commences at a temperature as low as about 150 °C.[14b] Indeed, poly(1-hexyne) is so unstable that it decomposes even at room temperature, as evidenced by the drastic decrease in its molecular weight after it has been put on shelf for a couple of days. In contrast, **P1** and

P2 lose 5% of their weights at temperatures as high as 365.8 and 377.7 °C, respectively (Supporting Information, Figure S8). The weight residues for **P1** and **P2** after pyrolysis at 800 °C are 66% and 63%, respectively. The thermogravimetric analysis data suggest that the multiple aromatic units in the pendants of the polymers have served as "radical sponges" to trap the detrimental species generated at high temperatures and that the network formation due to the thermally induced cross-linking reactions of the triple and/or double bonds have enhanced the resistance of the polymers to thermolysis.

As depicted in Figure 4, **P1** shows an absorption peak at 319 nm and a shoulder at 380 nm. The absorption peaks of its

Scheme 3. Synthesis of Conjugated Polyelectrolytes P1$^+$ and P2$^+$ via Quaternization of P1 and P2

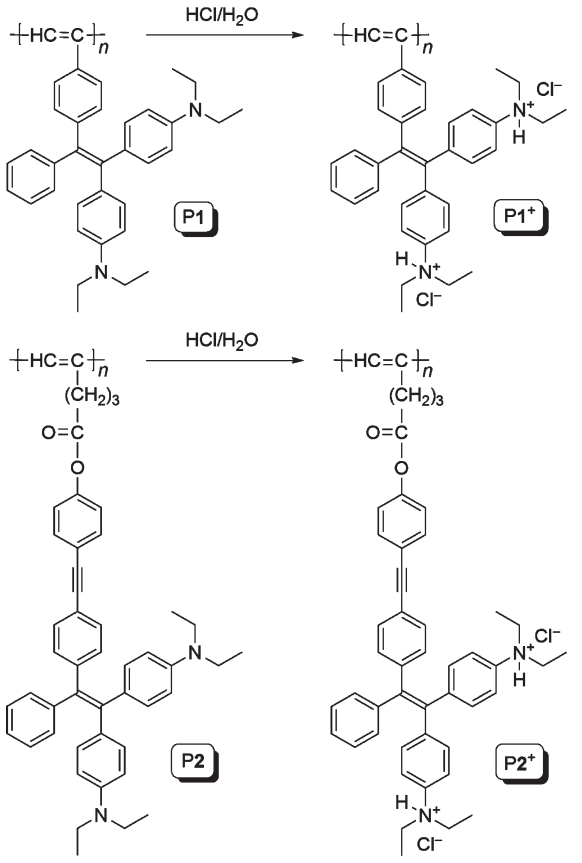

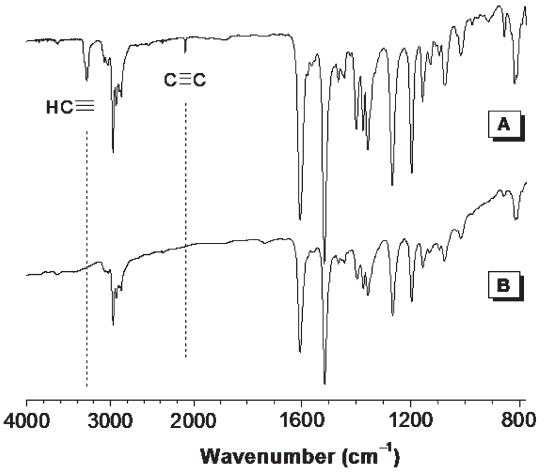

Figure 1. IR spectra of (A) monomer **1** and (B) its polymer **P1** (sample taken from Table 1, no. 5).

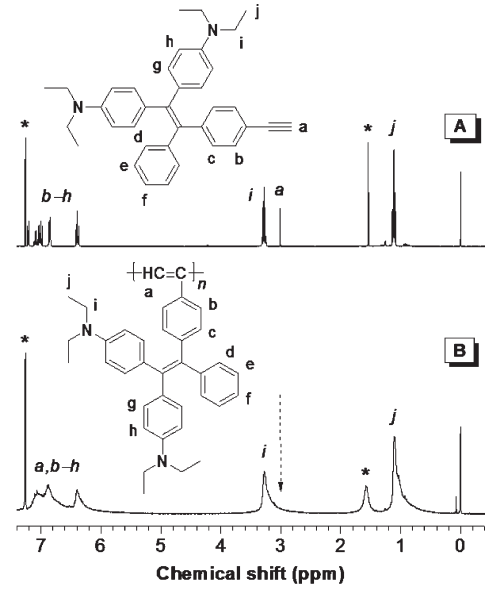

Figure 2. ^{1}H NMR spectra of (A) monomer **1** and (B) its polymer **P1** (sample taken from Table 1, no. 5) in chloroform-*d* at room temperature. The solvent and water peaks are marked with asterisks.

Table 1. Polymerizations of Monomers 1 and 2[a]

no.	catalyst	solvent	time (h)	yield (%)	M_w[b]	M_w/M_n[b]
			Monomer **1**			
1[c]	$[Rh(cod)Cl]_2$	THF	6			
2[c]	$[Rh(nbd)Cl]_2$	THF	6			
3[d]	$Rh^+(nbd)[C_6H_5B^-(C_6H_5)_3]$	THF	6	62.9	26 600	1.96
4	$[Rh(cod)Cl]_2$	THF/TEA	6	30.0	17 100	1.34
5	$[Rh(nbd)Cl]_2$	THF/TEA	6	60.1	48 100	1.58
6	$Rh^+(nbd)[C_6H_5B^-(C_6H_5)_3]$	THF/TEA	6	46.3	26 000	2.11
7	$[Rh(cod)Cl]_2$	THF/TEA	24	28.9	15 900	1.32
8	$[Rh(nbd)Cl]_2$	THF/TEA	24	57.9	61 200	1.65
9	$Rh^+(nbd)[C_6H_5B^-(C_6H_5)_3]$	THF/TEA	24	65.2	53 100	1.61
			Monomer **2**			
10	$[Rh(cod)Cl]_2$	THF/TEA	24	32.4	6 200	1.25
11	$[Rh(nbd)Cl]_2$	THF/TEA	24	30.5	16 100	2.86
12	$Rh^+(nbd)[C_6H_5B^-(C_6H_5)_3]$	THF	24	64.2	14 200	1.35

[a] Carried out under dry nitrogen at room temperature. $[M]_0$ = 0.1 M, [cat.] = 2 mM. Abbreviations: cod = 1,5-cyclooctadiene, nbd = 2,5-norbornadiene, THF = tetrahydrofuran, and TEA = triethylamine. [b] Estimated by GPC in THF on the basis of a polystyrene calibration. [c] No polymeric product isolated. [d] Data for the soluble fraction, for the polymerization product was only partially soluble in THF.

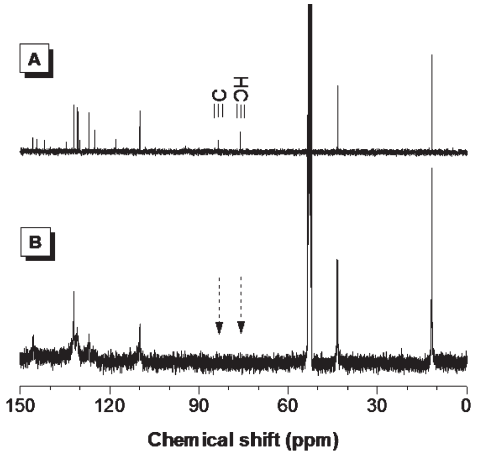

Figure 3. ^{13}C NMR spectra of (A) monomer **1** and (B) its polymer **P1** (sample taken from Table 1, no. 5) in DCM-d_2 at room temperature.

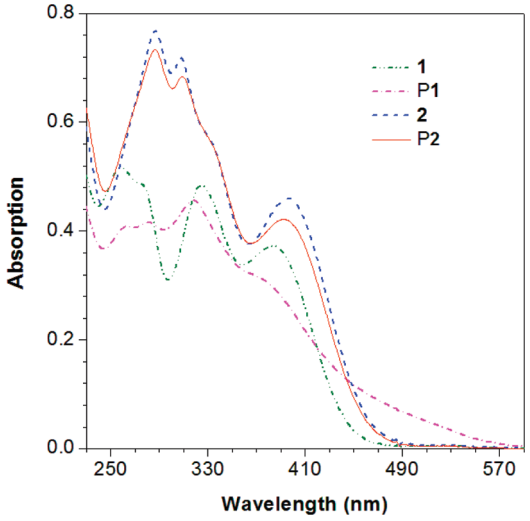

Figure 4. Absorption spectra of monomers **1** and **2** and their polymers **P1** and **P2** in THF at room temperature. Concentration (c): 20 μM.

monomer are located at similar wavelengths (325 and 383 nm), indicating that the peak and shoulder of **P1** are due to the absorption of its pendant groups. However, whereas the monomer does not absorb at wavelength longer than 490 nm, its polymer absorbs in the visible spectral region, with an absorption tail extending to ~600 nm. This suggests that the electronic communication between the aromatic pendants and the polyene backbone has enhanced effective conjugation length of **P1**. Little difference, however, is observed between the spectra of monomer **2** and its polymer **P2**, implying that the backbone absorption of the polymer is weak and overlapped with that of its pendants.

AIE Activity of Monomers. As can been seen from Figure 5A, monomer **1** is nonemissive when dissolved in THF but becomes luminescent when aggregated in THF/water mixtures with large fractions of water (f_w). Thus, similar to its parent form of TPE,[29] monomer **1** is AIE active. However, different from TPE, the emission peak of **1** drastically shifts with f_w. The solutions of **1** in THF and an aqueous mixture with f_w of 30% show barely discernible emission peaks at ~458 nm. The blue peak at 454 nm is greatly enhanced in the aqueous mixture with f_w of 80%, with two redder shoulder peaks appearing at 484 and 529 nm. When f_w is increased to 85%, the intensities of the peaks at 454 and 484 nm are

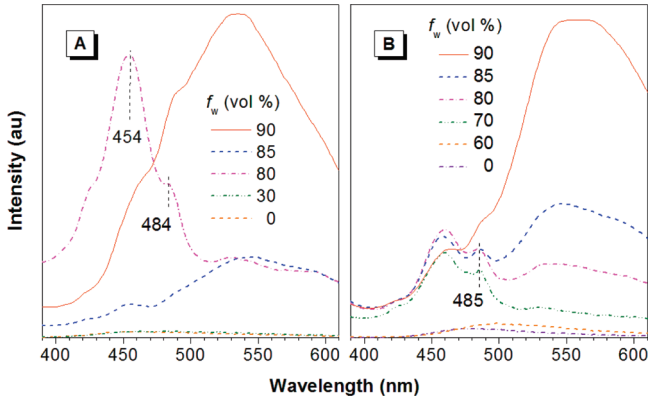

Figure 5. Emission spectra of (A) monomer **1** and (B) monomer **2** in THF/water mixtures with different fractions of water (f_w). Excitation wavelength (λ_{ex}): 320 nm; c = 40 μM.

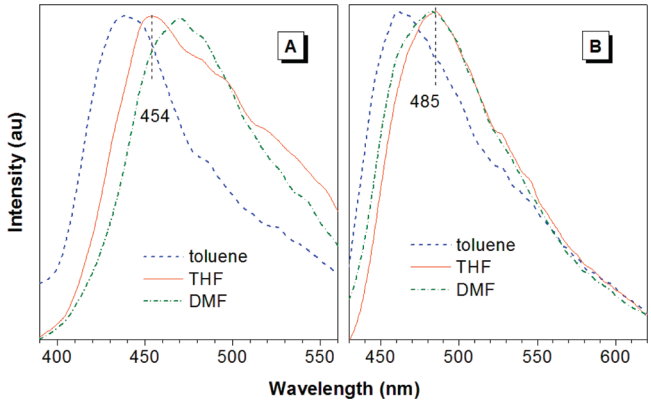

Figure 6. Emission spectra of (A) monomer **1** and (B) monomer **2** in toluene, THF, and DMF. Excitation wavelength: 320 nm for **1**; 400 nm for **2**; c = 20 μM.

decreased but that of the shoulder at 549 nm keeps nearly unchanged. Upon further increasing f_w to 90%, the emission spectrum is broadened, with the peak at 535 nm being significantly enhanced. Similarly, the emission of **2** is red-shifted and boosted with increasing f_w of the aqueous mixture (Figure 5B).

The emission behaviors of the monomers seem rather complex but are similar to our recently studied BODIPY derivatives with twisted intramolecular charge-transfer (TICT) characteristics.[39] It is well-known that emission spectrum of a TICT luminogen bathochromically shifts with an increase in solvent polarity. To examine whether monomers **1** and **2** are TICT active, we investigated the effect of solvent polarity on their emission behaviors. From the magnified and normalized emission spectra shown in Figure 6A, it can be clearly seen that the emission peak of monomer **1** is red-shifted when the solvent is changed from nonpolar toluene to polar *N*,*N*-dimethylformamide (DMF), thus confirming its TICT characteristic. The same change in solvent (toluene → DMF) brings about the analogous red shift in the emission spectrum of monomer **2** (Figure 6B).

On the basis of the experimental results, the emission behaviors of monomer **1** can be understood as follows. In THF, both of its locally excited (LE) and TICT states are nonemissive due to the active intramolecular rotations of its phenyl rings that consume its exciton energy via nonradiative channels. Addition of water, a nonsolvent of **1**, into THF increases the solvent polarity and decreases the solvating power. The former decreases the emission intensity of a

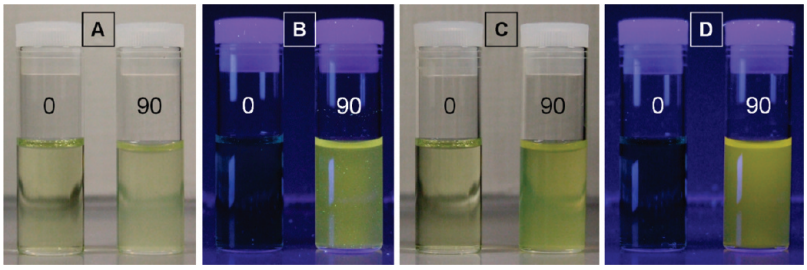

Figure 7. Photographs of monomers (A and B) **1** and (C and D) **2** in THF and THF/water mixture with 90 vol % water taken under (A and C) room lighting and (B and D) UV illumination (365 nm).

Chart 2. Antagonistic Effects of Water on Emission Efficiency of a Luminogen Solution[a]

[a] TICT = twisted intramolecular charge transfer, AIE = aggregation-induced emission.

TICT luminogen, whereas the latter promotes aggregate formation and activates AIE process; the emission of **1** is thus determined by the competition between these two antagonistic effects (Chart 2).[39] Because of the excellent solubility of **1** in THF, no aggregates are formed, and its emission intensity remains weak until a large amount of water is added into THF. When f_w is 80%, some molecules of monomer **1** start to aggregate and the emissions from both its LE (454 and 484 nm) and TICT (534 nm) states are enhanced, with the LE emission dominating the fluorescence spectrum. The TICT process prevails in the aqueous mixture with f_w of 85%, which greatly weakens the LE emission.[39] When f_w reaches 90%, the solvating power of the aqueous mixture becomes so poor that most or all of the luminogenic molecules now aggregate, which activates the AIE process and hence dramatically boosts the emission of **1**. The emission behaviors of **2** in the aqueous mixtures can be explained by the similar changes in the morphological structures and photophysical pathways.

Because of the total immiscibility of monomer **1** with water, its molecules must have aggregated in the THF/water mixture with 90% water. The aqueous suspension, however, is optically transparent and macroscopically homogeneous (Figure 7A), suggesting that the luminogen aggregates are nanosized, as is often the case in the TPE-based AIE systems.[29] No light emission from the THF solution of **1** can be observed by the naked eyes under UV illumination, but strong yellow light emission is seen from its nanoaggregate suspension in the 90% aqueous medium (Figure 7B). Similar behaviors are observed for the THF solution of **2** and its aqueous suspension (Figure 7, panels C and D).

AIE(E) Behaviors of Polymers. It becomes clear that the monomers are AIE-active. What kind of emission behaviors will their polymers show? To answer this question, we measured their emission spectra in THF and THF/water mixtures. We first studied the photophysical behaviors of **P1**. As can be seen from the spectrum shown in Figure 8A and the photograph given in Figure 8B, **P1** is faintly luminescent in THF, with an emission maximum at 613 nm. Since the emission of its parent form of poly(phenylacetylene) is peaked at ~500 nm,[40] the red-shifted emission (613 nm) of **P1** suggests that the polyacetylene backbone has conjugated with the TPE pendants, agreeing well with the UV spectral data. The low fluorescence efficiency is probably caused by the structural defects of the poly(phenylacetylene) skeleton

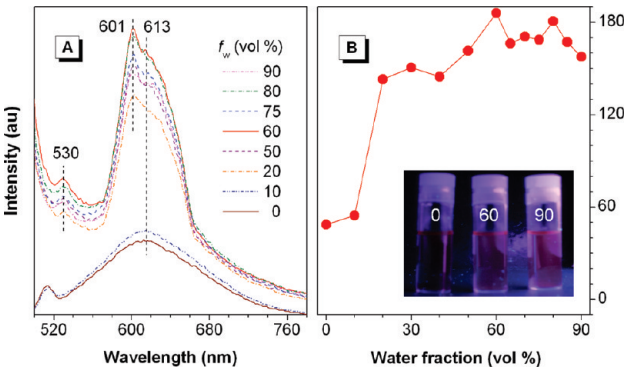

Figure 8. (A) Emission spectra of **P1** in THF/water mixtures with different fractions of water (f_w); λ_{ex} = 445 nm, c = 40 μM. (B) plot of emission intensity at 601 nm versus water fraction in the aqueous mixture. Inset: photographs of **P1** in the THF/water mixtures with f_w of 0, 60, and 90 vol % taken under illumination of a 365 nm UV light.

that has quenched the excitons through energy or electron transfer.[13,40,41] When water is added, the emission intensity of **P1** starts to increase from a much lower f_w (~20%), in comparison to that (~80%) in the case of its monomer (cf. Figure 5A). This is easy to understand because the polymer chains are much more hydrophobic than the monomer molecules and therefore have a much higher propensity to aggregate in a polar medium. The light emission of the polymer is therefore enhanced by aggregate formation, showing an AIEE effect. The extent of the enhancement, however, is limited: the maximum increase in the emission intensity is ~2.8-fold, as can be seen from Figure 8.

It is noticeable that in the THF/water mixture containing 20% water a new emission peak appears at 601 nm, besides the original peak at 613 nm in pure THF. It is suspected that a TICT−LE transition is involved in the system of **P1**: upon aggregate formation, the surrounding environment of some polymer chains becomes more hydrophobic because they are separated or shielded from the polar solvent, which thus blue-shifts the polymer emission.[39] To validate this hypothesis, the solvent effect on the emission of **P1** is examined. As shown in Figure 9, the maximum emission peaks locate at 605, 613, and 630 nm in toluene, THF, and DMF, respectively. The hypsochromically shifted emission spectrum of **P1** in the less polar solvent thus verifies our assumption.

It is also noticed that there are small peaks at 530 nm in the emission spectra of **P1** in the aqueous mixtures (cf. Figure 8A). The peak is probably associated with the TICT emission of the TPE unit, which appears at ~529 nm in the THF/water mixtures (cf. Figure 5A). It seems that there are emission peaks in the wavelength region below 500 nm, which overlap with the light from the excitation source. To clarify this issue, the excitation wavelength is changed from 445 to 365 nm, and the results are shown in Figure 10.

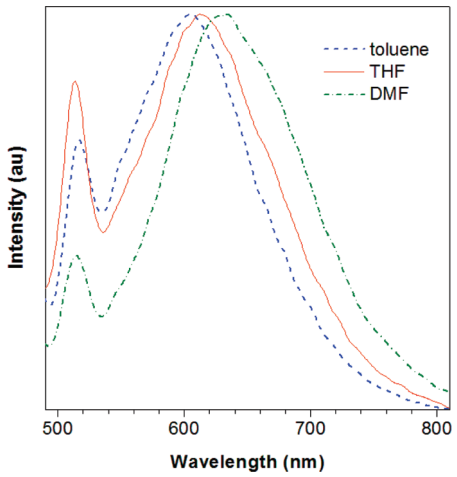

Figure 9. Emission spectra of **P1** in different solvents. c = 20 μM, λ_{ex} = 445 nm.

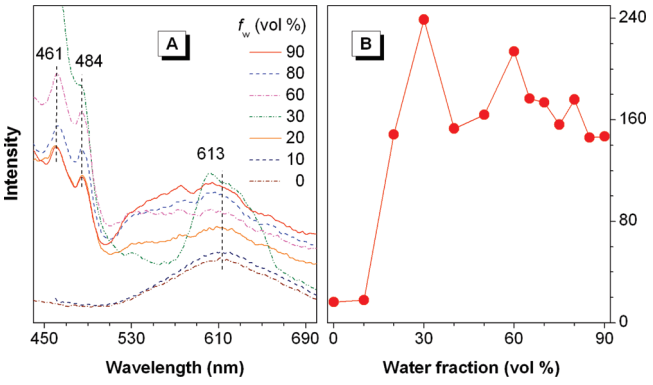

Figure 10. (A) Emission spectra of **P1** in THF/water mixtures with different fractions of water (f_w). λ_{ex} = 365 nm, c = 40 μM. (B) Plot of emission intensity at 484 nm versus water fraction in the aqueous mixture.

Indeed, two distinct peaks appear at 461 and 484 nm, which should be associated with the LE emission of the TPE pendants (cf. Figure 5A). Another broad peak in the wavelength region from 510 nm to over 700 nm is also seen, which should be the merged emissions of the TICT states of the polymer chains and pendants. Figure 10B shows the plot of the emission intensity versus the water fraction at 484 nm. Clearly, the LE emission of the TPE pendant changes in a way similar to that of the polymer chain (cf. Figure 8B) but with a much higher extent of enhancement (13.5-fold).

P1 is an AIEE polymer with a low emission efficiency, which is determined by its molecular structure. The direct link of the TPE units with the polyene backbone restricts the intramolecular rotations of the pendants, making the polymer luminescent even in the solution. The poly(phenylacetylene) skeleton, on the other hand, has structural defects that trap the excitons and decrease the emission efficiency. The outcome of these two opposite effects is the weak emission of **P1** in the THF solution. **P2** differs from **P1**, in that the polymer backbone and the TPE pendants are separated by flexible alkyl spacers, which provide enough freedom for the pendants to undergo intramolecular rotations. Furthermore, **P2** is a poly(1-alkyne) derivative, whose skeleton is harmless to light emission.[41] Owing to these reasons, **P2** is potentially AIE-active. Indeed, **P2** shows a typical AIE behavior. As can be seen from Figure 11A, the polymer is practically nonluminescent in THF. However, its emission intensity is

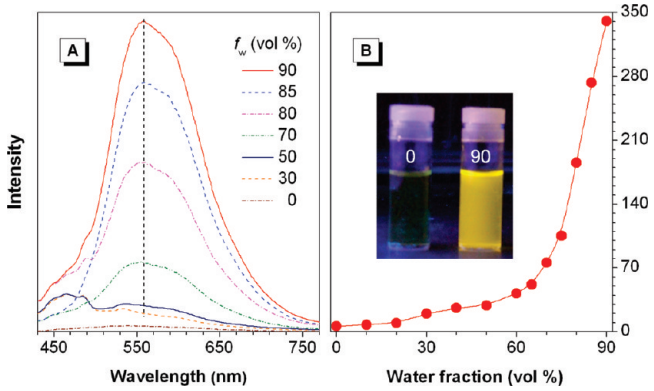

Figure 11. (A) Emission spectra of **P2** in THF/water mixtures with different fractions of water (f_w). λ_{ex} = 400 nm, c = 40 μM. (B) Plot of emission intensity at 558 nm versus water fraction in the aqueous mixture. Inset: photographs of **P2** in the THF/water mixtures with f_w (vol %) of 0 and 90 taken under UV illumination.

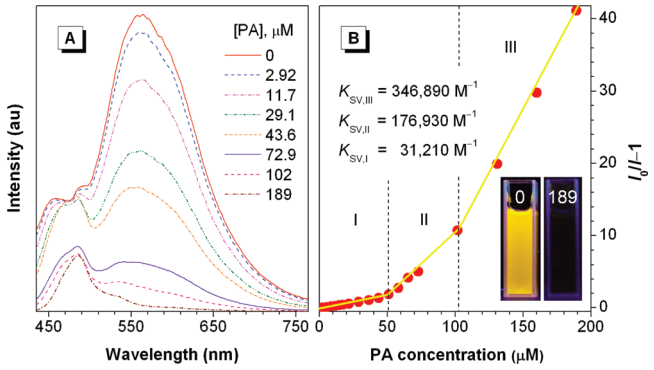

Figure 12. (A) Emission spectra of **P2** (40 μM) in a THF/water mixture (f_w = 90%) in the presence of different amounts of picric acid (PA); λ_{ex} = 400 nm. (B) Stern−Volmer plot of $I_0/I - 1$ versus PA concentration in the aqueous mixture and K_{sv} values (in unit of M^{-1}) in different concentration regions, where I_0 is the emission intensity of **P2** in the absence of PA. Inset: photographs of **P2** in the aqueous mixtures containing 0 and 189 μM PA.

gradually increased with increasing water content in the THF/water mixture. The increase becomes faster when f_w is increased to ~75% (Figure 11B). In the 90% aqueous mixture, the maximum emission intensity of the polymer nanoaggregates is >56-fold higher than that in the THF solution.

Explosive Detection by P2 Nanoaggregates. The strong light emissions of the nanoaggregates of **P2** suspended in the aqueous mixtures prompted us to explore its potential applications as chemosensors. The sensitive detection of explosives, such as 2,4-dinitrotoluene, 2,4,6-trinitrotoluene, and picric acid (PA), has aroused much interest because of its antiterrorism implications. We explored the possibility of using the emissive nanoaggregates of **P2** in the 90% aqueous mixture as an explosive probe. Because of its commercial availability, PA is chosen as a model explosive in this study. As can be seen from Figure 12A, the emission of the nanoaggregates is weakened when PA is added. The emission quenching can be observed at a PA concentration as low as 0.72 μM or 0.17 ppm. At a PA concentration of 189 μM, the emission from the nanoaggregates becomes so weak that it cannot be observed by the naked eyes (Figure 12B, inset).

The Stern−Volmer plot for the emission quenching of **P2** nanoaggregates suspended in the aqueous medium by PA is shown in Figure 12B, from which the Stern−Volmer constant (K_{SV}) or quenching efficiency can be determined.

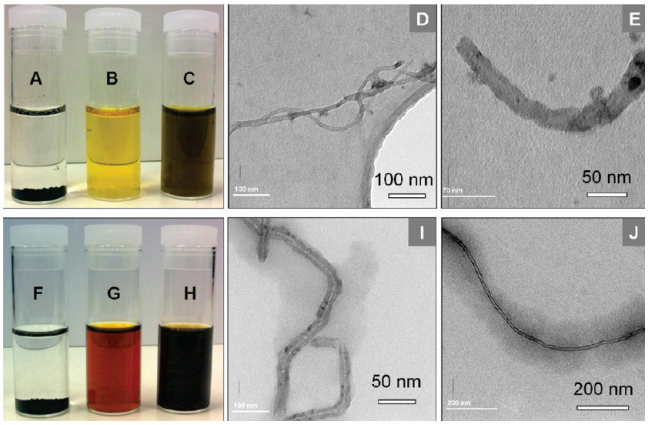

Figure 13. Photographs of (A) pristine MWNTs, (B) $\mathbf{P1}^+$, and (C) $\mathbf{P1}^+$/MWNT hybrid in water and (F) pristine MWNTs, (G) **P1**, and (H) **P1**/MWNT hybrid in THF. Transmission electron microscope (TEM) images of (D, E) $\mathbf{P1}^+$/MWNT and (I, J) **P1**/MWNT hybrids.

Intriguingly, the plot is composed of three stages. In stage I or in the low concentration region with [PA] $\leq$ 51 μM, the plot is linear with a $K_{SV,I}$ value of 31 210 M^{-1}. When the explosive concentration is increased to $>$51 μM, the Stern−Volmer plot is deviated from the linear one for the low [PA] region and enters stage II, where the plot follows another linear relationship with a 5.7-fold higher quenching efficiency ($K_{SV,II}$ = 176 930 M^{-1}). In stage III or in the very high quencher concentration region ([PA] $>$ 102 μM), the plot follows yet another linear equation with a $K_{SV,III}$ value as high as 346 890 M^{-1}.

Many fluorescent polymers have been used as chemosensors for explosive detections. For example, polymetalloles such as polysiloles and polygermoles have been utilized to probe explosives such as PA in THF and toluene solutions. The K_{SV} values for the PA assay have been found to be in the range of 6710−11 000 M^{-1} in the concentration range of 0−0.2 mM.[42] The $K_{SV,I}$ value for the PA detection by the nanoaggregates of **P2** in the lowest concentration region (0−51 μM) is already 2.8-fold higher than the highest quenching efficiency achievable by the polymetalloles.[42] The K_{SV} value is increased with increasing quencher concentration, and the quenching efficiency in stage III becomes 31.5-fold higher than that in the polymetallole system. This set of continuously increasing K_{SV} values is indicative of a novel superamplification effect in the emission quenching process. When a PA molecule penetrates into the three-dimensional network of a nanoaggregate of **P2** suspended in the aqueous medium, it may quench the light emission of multiple luminogenic species in the vicinity. This makes the fluorescence of the nanoaggregates of the polymer highly susceptible to the quencher concentration, thus resulting in the observed superquenching effect.

Hybridization of CPEs with CNTs. CPEs bearing ionic pendants are soluble in high dielectric media. The polymers exhibit unique solution properties and have found useful optical, photonic, and biosensory applications.[34,36] **P1** and **P2** are conjugated polymers carrying basic amino pendant groups, which can be facilely ionized by an acid, leading to the formation of water-soluble CPEs. Thus, **P1** and **P2** are transformed to their corresponding polyelectrolytes $\mathbf{P1}^+$ and $\mathbf{P2}^+$, respectively, by simply stirring their mixtures with hydrochloric acid in water at room temperature for ~15 min, as evidenced by the complete dissolution of the originally hydrophobic polyacetylenes in the aqueous medium after the quaternization (cf. Scheme 3).

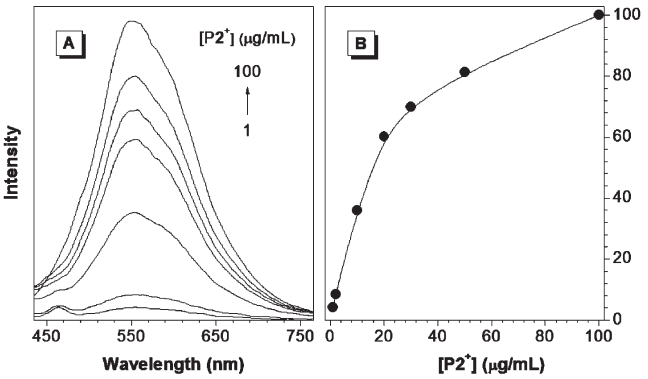

Figure 14. (A) Emission spectra of $\mathbf{P2}^+$ in aqueous phosphate buffer (pH = 7.0) at different polymer concentrations; λ_{ex} = 400 nm. (B) Effect of polymer concentration on the emission intensity at 551 nm.

In our previous studies, we have found that poly(phenylacetylene) derivatives are good dispersants for carbon nanotubes (CNTs) in solvents due to the $\pi-\pi$ interactions of the poly(phenylacetylene) skeleton and its aromatic pendants with the CNT walls.[19c,25,41b] $\mathbf{P1}^+$ is thus anticipated to be capable of dispersing CNTs in aqueous media. Indeed, highly soluble $\mathbf{P1}^+$/MWNT nanohybrids are formed when $\mathbf{P1}^+$ and multiwalled carbon nanotubes (MWNTs) are admixed in water. Figure 13 shows the photographs of MWNTs, $\mathbf{P1}^+$, and $\mathbf{P1}^+$/MWNT nanohybrid in water. Clearly, after hybridization with $\mathbf{P1}^+$, the originally totally immiscible MWNT agglomerates (Figure 13A) become soluble, giving a dark brown aqueous solution (Figure 13C). The solubility of MWNTs in water is evaluated by our previously published method[19c,25d] to be as high as 430 mg/L, indicating that $\mathbf{P1}^+$ is a good dispersant for MWNTs.

For comparison, the analogous hybridization experiment was performed for **P1** and MWNTs in THF. As can be seen from Figure 13H, **P1** and MWNTs can also form highly dispersible nanohybrids. The solvating power of **P1** for MWNTs in THF is ~630 mg/L, even higher than that of its CPE counterpart in the aqueous media. This is probably due to the repulsive electrostatic interactions between the CPE chains carrying the same positive charges, which have prevented the polyelectrolyte chains from further wrapping the already formed $\mathbf{P1}^+$/MWNT hybrids, thus diminishing its solvating power for MWNTs. Transmission electron microscope (TEM) images clearly show that the MWNTs are coated by the polymer chains. Noticeably, the polymer coatings in the **P1**/MWNT nanohybrids (Figure 13, panels I and J) are more obvious and thicker than those in the $\mathbf{P1}^+$/MWNT nanohybrids (Figure 13, panels D and E), consistent with the solubility data.

Protein Quantitation by $\mathbf{P2}^+$. To check whether $\mathbf{P2}^+$ is AIE active, we investigated its emission behaviors in the solution and solid states. The polymer is nonemissive in dilute solution but becomes emissive in solid state, showing a characteristic AIE behavior. To collect more information about its photophysical properties, the effect of concentration on the emission of $\mathbf{P2}^+$ is studied. As shown in Figure 14, when its concentration in the aqueous buffer is increased from 1 to 100 μg/mL, its emission intensity is enhanced by 24 times. For the purpose of comparison, the emission spectra of its monomer $\mathbf{2}^+$ (Supporting Information, Chart S1) in the aqueous buffer at different concentrations are taken. As can be seen from Figures S10 and S11 shown in the Supporting Information, the emission intensity of $\mathbf{2}^+$ is linearly increased with the luminogen concentration.

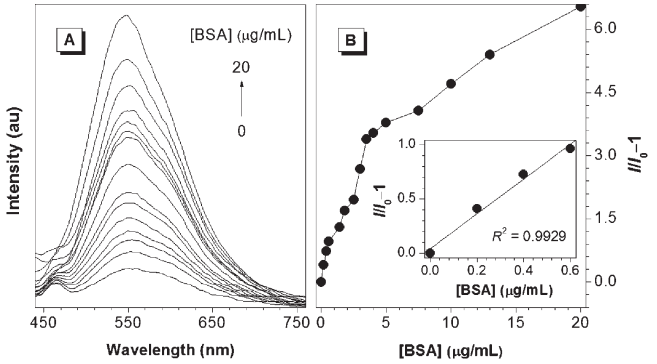

Figure 15. (A) Emission spectra of $\mathbf{P2}^+$ (2 μg/mL) in an aqueous phosphate buffer (pH = 7) containing different amounts of bovine serum albumin (BSA); λ_{ex} = 400 nm. (B) Plot of $I/I_0 - 1$ versus concentration of BSA, where I_0 is the emission intensity of $\mathbf{P2}^+$ at 548 nm in the absence of BSA. Inset: enlarged portion of the plot in the low concentration region.

To gain further insights into the fluorescence processes of $\mathbf{2}^+$ and $\mathbf{P2}^+$, the concentration effects on the light emissions of their neutral counterparts **2** and **P2** in THF are investigated. As shown in Figure S12 (Supporting Information), neither of them is emissive even when their concentrations are increased to 100 μg/mL. Because the neutral (macro)-molecules are highly soluble in THF, they are well dispersed in the good solvent even at the high concentrations, which accounts for the nil concentration effects on their emission intensities. The amphiphilic (macro)molecules of $\mathbf{2}^+$ and $\mathbf{P2}^+$, however, are dissolved in the aqueous medium at the low concentrations but form nanoaggregates or micelle-like assemblies due to the hydrophobic interactions between their aromatic chromophores at the high concentrations. The covalent attachment of the luminogenic units to the polymer chains and the steric effect induced by the repulsive electrostatic interaction between the cationic luminogens rigidifies their molecular structures, which further restricts their intramolecular rotations and hence makes the CPE aggregates formed at the high concentrations fluorescent.

CPEs have been widely used as chemical sensors and biological probes.[34,36] The "traditional" CPE bioprobes usually operate in a light "turn-off" mode[10,34] due to the emission quenching caused by the electron and/or energy transfers between the CPE chains and the bioanalytes. It will be better if the bioprobes can work in a fluorescence "turn-on" mode, which enjoy such advantages as high detection sensitivity, reduced false-positive signals, and visual recognition or discrimination with the naked eyes. AIE-active CPEs may serve as such turn-on biological probes. Upon conjugating with bioanalytes, the intramolecular rotations in the CPE luminogens will be restricted, which will in turn activate the light emission processes of the nonemissive polymers. $\mathbf{P2}^+$ is an AIE-active CPE, and it is thus expected that it will function as a "light-up" bioprobe.

$\mathbf{P2}^+$ is positively charged and should show affinity toward negatively charged biopolymers. Bovine serum albumin (BSA) is an electronegative protein, to which $\mathbf{P2}^+$ may bind. To explore the possibility of utilizing $\mathbf{P2}^+$ for protein assay, its emission spectra in the absence and presence of BSA are measured. In the absence of BSA and at a low luminogen concentration ([$\mathbf{P2}^+$] = 2 ppm) in the aqueous buffer, the polymer is weakly luminescent (Figure 15A). Addition of a tiny amount of protein ([BSA] = 0.2 ppm) results in an immediate increase in the emission intensity, indicating that $\mathbf{P2}^+$ can be employed for trace analysis of protein. The emission is progressively intensified with gradual addition of BSA into the aqueous solution of $\mathbf{P2}^+$. At 20 μg/mL of BSA, the emission is increased by ~7.5 times. In the BSA concentration range of 0−0.6 μg/mL, the $I/I_0 - 1$ vs [BSA] plot follows a linear relationship with an outstanding "goodness-of-fit" (R^2 = 0.9929; Figure 15B), demonstrating that $\mathbf{P2}^+$ can function as a biological probe for BSA quantification at subppm level.

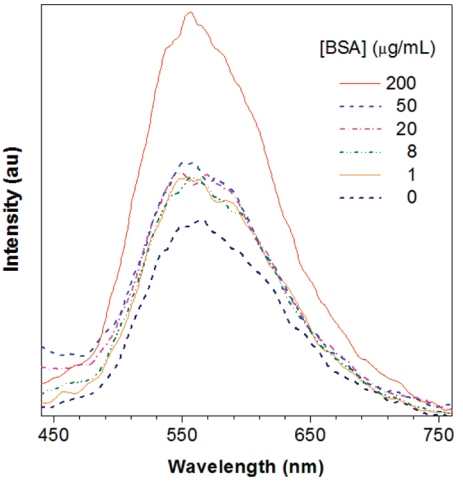

Figure 16. Emission spectra $\mathbf{2}^+$ (2 μg/mL) in an aqueous phosphate buffer (pH = 7) containing different amounts of BSA. λ_{ex} = 400 nm.

Monomer $\mathbf{2}^+$ does not perform as well as does its polymer $\mathbf{P2}^+$. As shown in Figure 16, some small increments in the emission of $\mathbf{2}^+$ are observed in the BSA concentration range of 1−50 μg/mL. Even when a very large amount of BSA (200 μg/mL) is added into the monomer solution, the increase in the emission intensity is still rather low ($I/I_0 \sim 2$). These results suggest that the stringing together of the multiple TPE units in a macromolecule chain greatly enhances its sensitivity to protein. The binding of one luminogen pendant in $\mathbf{P2}^+$ to a BSA chain may induce a large chain segment of $\mathbf{P2}^+$ or even a whole CPE chain to dock on the surface of the folding structure of the protein in the aqueous medium. This cooperative effect may account for the significantly amplified response of the polymer emission to the protein analyte.[19b,21,41,43]

Concluding Remarks

In this work, acetylene monomers functionalized by aminated TPE groups **1** and **2** are synthesized and successfully transformed to their corresponding polymers **P1** and **P2** by organorhodium complexes. The polymer chains possess unusual *E* conformation, possibly due to the anchoring effect of the functional amino groups in the monomers in the polymerization reactions. While **P1** shows an AIEE behavior, **P2** is AIE-active. The emission of **P2** nanoaggregates suspended in the aqueous medium is quenched by PA in high efficiency and the K_{SV} value is nonlinearly increased with increasing PA concentration over a wide concentration range, showing an intriguing superamplification effect. The quaternization by acid readily transforms the organic solvent-soluble polymers **P1** and **P2** to the aqueous medium-miscible CPEs $\mathbf{P1}^+$ and $\mathbf{P2}^+$, respectively. Nanohybrids of $\mathbf{P1}^+$ and MWNTs are prepared by simply mixing the two components in water. $\mathbf{P2}^+$ functions as a fluorescence turn-on bioprobe, allowing quantitation of BSA in sub-ppm concentration region. The high sensitivity of the CPE is probably stemmed from a cooperative effect in the binding process between $\mathbf{P2}^+$ and BSA chains.

Experimental Section

Materials and Instruments. THF was distilled under normal pressure from sodium benzophenone ketyl under argon immediately

prior to use. TEA was distilled and dried over potassium hydroxide. DCM was distilled over calcium hydride under nitrogen before use. Other solvents, such as pyridine, hexane, and ethyl ether, are of high purities and were used as received. 4-Bromobenzophenone (**3**), (trimethylsiyl)acetylene (**4**), 4,4′-bis(diethylamino)benzophenone (**6**), 4-iodophenol (**8**), 5-hexynoic acid (**10**), dichlorobis(triphenylphosphine)palladium(II), copper(I) iodide, triphenylphosphine, zinc dust, titanium tetrachloride, *p*-toluenesulfonic acid monohydrate (TsOH), *N,N′*-dicyclohexylcarbodiimide (DCC), 4-(dimethylamino)pyridine (DMAP), and 1 M tetrabutylammonium fluoride (TBAF) in THF with 5% water were purchased from Aldrich and used without further purification. Rhodium complexes $[Rh(cod)Cl]_2$, $[Rh(nbd)Cl]_2$ and $Rh^+(nbd)[C_6H_5B^-(C_6H_5)_3]$ were prepared in our laboratories following the literature methods.[44,45] BSA was purchased from Sigma and stored in a cold, dark place before use. Phosphate buffer solution with pH = 7.0 was purchased from Merck.

^1H and ^{13}C NMR spectra were measured on a Bruker ARX 400 spectrometer using chloroform-*d*, DMSO-d_6 as solvent and tetramethylsilane (TMS) as internal standard. Matrix-assisted laser desorption/ionization time-of-flight (MALDI-TOF) high-resolution mass spectra (HRMS) were recorded on a GCT premier CAB048 mass spectrometer. Absorption spectra were taken on a Milton Roy Spectronic 3000 Array spectrometer. Emission spectra were taken on Perkin-Elmer spectrofluorometer LS 55. Molecular weights (M_w and M_n) and polydispersity indexes (M_w/M_n) of the polymers were estimated by a Waters Associates gel permeation chromatography (GPC) system in THF. A set of monodisperse polystyrene standards covering molecular weight range of 10^3-10^7 was used for molecular weight calibration. TEM images were obtained on a JEOL/JEM-200 CX microscope coupled with an EDX analyzer.

Preparations of Monomers. Monomers **1** and **2** were prepared according to the synthetic routes shown in Schemes 1 and 2, respectively. The detailed experimental procedures and characterization data are given below.

Preparation of 4-[2-(Trimethylsilyl)ethynyl]benzophenone (**5**). Into a 100 mL two-necked flask were added 70.1 mg (0.1 mmol) of $PdCl_2(PPh_3)_2$, 19 mg (0.1 mmol) of CuI, 13 mg (0.05 mmol) of PPh_3, 1.3 g of 4-bromobenzophenone (**3**; 5 mmol), and a mixture of 55 mL of THF/TEA (5:50 v/v) under nitrogen. After the catalysts were completely dissolved, 0.9 mL (6.5 mmol) of (trimethylsiyl)acetylene (**4**) was injected into the flask, and the mixture was stirred at 50 °C for 24 h. The formed solid was removed by filtration and washed with diethyl ether. The filtrate was concentrated by a rotary evaporator. The crude product was purified on a silica gel column with chloroform/hexane (1:1 by volume) as eluent. A pale brown solid was obtained in 85.5% yield. IR (KBr), ν (cm^{-1}): 2158 (m, C≡C), 1649 (vs, C═O). ^1H NMR (400 MHz, $CDCl_3$), δ (TMS, ppm): 7.78, 7.76, 7.74, 7.57, 7.55, 7.48 (m, 9H, aromatic protons), 0.27 (s, 9H, $Si(CH_3)_3$). ^{13}C NMR (100 MHz, $CDCl_3$), δ (TMS, ppm): 195.93 (C═O), 137.38, 136.97, 132.53, 131.77, 129.94, 129.88, 128.34, 127.33, 104.06 (≡C−Ar), 97.83 (≡C−Si), −0.17 ($-Si(CH_3)_3$). HRMS (MALDI-TOF): Calcd for $C_{18}H_{18}OSi$: 278.1127. Found: 277.1853 [$(M - H)^+$].

Synthesis of 1,1-Bis(4-(diethylamino)phenyl)-2-(4-(2-(trimethylsilyl)ethynyl)phenyl)-2-phenylethylene (*7*). Into a 250 mL two-necked round-bottom flask equipped with a reflux condenser was placed 0.507 g of zinc dust (7.6 mmol). The flask was evacuated under vacuum and flushed with dry nitrogen three times, after which 80 mL of THF was added. The mixture was cooled to around −5 °C, to which 0.42 mL of titanium tetrachloride was slowly added. The mixture was slowly warmed to room temperature and stirred for 0.5 h and then refluxed for 2.5 h. The mixture was again cooled to around −5 °C, charged with 0.16 mL of pyridine, and stirred for 10 min. Then 20 mL of a THF solution of 0.835 g of **5** (3 mmol) and 4,4′-bis-(diethylamino)benzophenone (**6**; 1.07 g, 3.3 mmol) was added slowly. The mixture was refluxed overnight. The reaction was quenched with a 10% potassium carbonate aqueous solution. A large amount of water was added until the solid is turned to gray or white. The mixture was then extracted with DCM three times, and the combined organic layer was washed by brine twice. The mixture was dried over 5 g of anhydrous sodium sulfate for 4 h. The crude product was condensed and purified on a silica gel column using gradient eluent from hexane to DCM/hexane (1:1 by volume). A yellow solid was obtained in 69.3% yield. IR (KBr), ν (cm^{-1}): 2153 (m, C≡C). ^1H NMR (400 MHz, $CDCl_3$), δ (TMS, ppm): 7.18, 7.06, 7.01, 6.98, 6.96, 6.87, 6.83, 6.39, 6.36 (18H, aromatic protons), 3.28 (m, 8H, $-(NCH_2)_4$), 1.12 (m, 12H, $-(CH_3)_4$). HRMS (MALDI-TOF): Calcd for $C_{39}H_{46}N_2O$: 570.3430. Found: 570.4491 [M^+].

Synthesis of 1,1-Bis[4-(diethylamino)phenyl]-2-(4-ethynylphenyl)-2-phenylethylene (*Monomer 1*). Into a 100 mL round-bottom flask was placed 20 mL of a THF solution of **7** (1.14 g, 2 mmol) and 3 mL of 1 M TBAF. After stirring for 45 min, 60 mL of water was added. The mixture was extracted with 200 mL of DCM three times, and the DCM solution was washed by brine twice. The mixture was then dried over 5 g of anhydrous sodium sulfate for 4 h. The crude product was condensed and purified on a silica gel column using a mixture of DCM/hexane (1:1 by volume) as eluent. A yellow solid of **1** was obtained in 89.3% yield. IR (KBr), ν (cm^{-1}): 3285 (s, HC≡), 2104 (m, C≡C). ^1H NMR (400 MHz, $CDCl_3$), δ (TMS, ppm): 7.20, 7.10, 7.08, 7.04, 7.03, 7.01, 7.00, 6.98, 6.86, 6.84, 6.39 (18 H, aromatic protons), 3.28 (m, 8H, $-(NCH_2)_4$), 3.01 (s, 1H, HC≡), 1.12 (m, 12H, $-(CH_3)_4$). ^{13}C NMR (100 MHz, $CDCl_3$), δ (TMS, ppm): 146.42, 145.15, 142.55, 135.15, 132.87, 131.62, 131.52, 131.36, 130.88, 130.77, 127.60, 125.49, 118.41, 110.78, 84.37, (Ar−C≡), 44.15 ($-CH_2$), 13.33 ($-CH_3$). HRMS (MALDI-TOF): Calcd for $C_{36}H_{38}N_2$: 498.3035. Found: 498.1895 [M^+].

Preparation of 1,1-Bis(4-(diethylamino)phenyl)-2-(4-(2-(4-phenolyl)ethynyl)phenyl)-2-phenylethylene (*9*). Into a 100 mL two-necked round-bottom flask were added 41 mg of $Pd(PPh_3)_4$, 7 mg of CuI, 1.010 g of **1**, 0.489 g of 4-iodiophenol, and a mixture of 55 mL of THF/TEA (5:50 v/v) under nitrogen. The mixture was stirred at room temperature for 24 h. The formed solid was removed by filtration and washed with diethyl ether. The filtrate was then concentrated by a rotary evaporator. The crude product was purified by recrystallization in a DCM/hexane mixture. A yellow solid was obtained in 60.5% yield. IR (KBr), ν (cm^{-1}): 3225 (w, broad, OH), 2211 (w, C≡C). ^1H NMR (400 MHz, $CDCl_3$), δ (TMS, ppm): 7.37, 7.21, 7.08, 7.05, 7.02, 7.00, 6.79, 6.40 (21H, aromatic protons), 4.99 (s, broad, −OH), 3.28 (m, 8H, $-(NCH_2)_4$), 1.12 (m, 12H, $-(CH_3)_4$). HRMS (MALDI-TOF): Calcd for $C_{42}H_{42}N_2O$: 590.3297. Found: 591.2526 [$(M + H)^+$].

Synthesis of 4-[2-(4-{2,2-Bis[4-(diethylamino)phenyl]-1-phenylvinyl}phenyl)ethynyl]phenyl 5-Hexynoate (*Monomer 2*). Into a 100 mL round-bottom flask were placed 566.8 mg (1 mmol) of **9**, 123 mg (1.1 mmol) of 5-hexynoic acid (**10**), 412 mg (2 mmol) of DCC, 24.4 mg (0.2 mmol) of DMAP, and 38.0 mg (0.2 mmol) of TsOH in 60 mL of DCM. The resultant mixture was stirred for 24 h at room temperature. After filtering the urea salts formed during the reaction, the solid was wash with diethyl ether and the filtrate was concentrated by a rotary evaporator. The product was purified by a silica gel column using a mixture of DCM/hexane (5:1 v/v) as eluent. A pale orange solid of **2** was obtained in 74.7% yield. IR (KBr), ν (cm^{-1}): 3297 (HC≡C), 2215 (C≡C), 2118 (C≡C), 1762 (C═O). ^1H NMR (400 MHz, $CDCl_3$), δ (TMS, ppm): 7.48, 7.23, 7.07, 7.05, 6.87, 6.40 (aromatic protons), 3.29 (m, 8H, $-(NCH_2)_4$), 2.72 (t, 2H, O═CCH_2), 2.36 (m, 2H, CH_2C≡), 2.02 (t, 1H, HC≡), 1.97 (m, 2H, O═C$CH_2C\mathit{H}_2$), 1.13 (m, 12H, $-(CH_3)_4$). ^{13}C NMR (100 MHz, $CDCl_3$), δ (TMS, ppm): 171.28 (C═O), 150.21, 146.53, 146.19, 145.22, 142.47, 132.90, 132.60, 131.65, 130.94, 127.59, 125.47, 121.57, 121.27, 110.76, 90.23, 88.18, 82.99 ($CH_2C\mathit{\equiv}$), 69.43 (HC≡), 44.15 ($-CH_2$), 32.93 ($-CH_2\mathit{C}H_2CH_2$), 23.45 (O═C$\mathit{C}H_2$), 17.80 (HC≡$\mathit{C}\mathit{C}H_2$), 12.65, ($-CH_3$). HRMS (MALDI-TOF): Calcd for $C_{48}H_{48}N_2O_2$: 684.3716. Found: 684.3754 [M^+].

Syntheses of Polymers. All the polymerization reactions and manipulations were carried out under nitrogen using Schlenk technique in a vacuum-line system except for the purification of the resultant polymers, which was done in an open atmosphere. The synthetic routes to the polymers are shown in Schemes 1 and 2. Typical experimental procedures for the polymerization of monomer **2** in THF using $Rh^+(nbd)[C_6H_5B^-(C_6H_5)_3]$ as catalyst are given below as an example.

In a 20 mL Schlenk tube with a side arm was placed 132 mg (0.2 mmol) of **2**. The tube was evacuated under vacuum and then flushed with nitrogen three times through the side arm. Then 1 mL of THF was injected. The catalyst solution was prepared in another Schlenk tube by dissolving 2.3 mg of $Rh^+(nbd)$-$[C_6H_5B^-(C_6H_5)_3]$ in 1 mL of THF. After aging for 15 min, it was transferred to the monomer solution using a hypodermic syringe. The reaction mixture was stirred at room temperature under nitrogen for 24 h. The resulting mixture was diluted with 5 mL of THF and added dropwise through a cotton filter into 500 mL of methanol under stirring. The precipitate was allowed to stand for 24 h and then filtered with a Gooch crucible. The polymer was washed with methanol five times and dried in a vacuum oven at 40 °C to a constant weight.

Characterization Data for P1 (*Table 1, No. 5*). Black solid; yield: 60.1%. M_w: 48 100, M_w/M_n: 1.58. IR (KBr), ν (cm^{-1}): 2965, 1374, 1356, 1265, 1194, 1154, 1076, 1016, 813, 699. ^1H NMR (400 MHz, $CDCl_3$), δ (TMS, ppm): 7.06, 6.89, 6.42, 3.28 (8H, $(-NCH_2)_4$), 1.11 (12H, $-(CH_3)_4$). ^{13}C NMR (100 MHz, $CDCl_3$), δ (TMS, ppm): 146.25, 132.84, 131.67, 127.51, 110.78, 44.17 ($-CH_2$), 12.64 ($-CH_3$).

Characterization Data for P2 (*Table 1, No. 12*). Yellow solid; yield: 64.2%. M_w: 14 200, M_w/M_n: 1.35. IR (KBr), ν (cm^{-1}): 2969, 2930, 2870, 2214 (very weak but cognizable, stretching vibration of C≡C attached to phenyl), 1759 (C=O), 1605, 1515, 1399, 1374, 1356, 1205, 1195, 1164, 1120, 1076, 1016, 763, 699, 669. ^1H NMR (400 MHz, $CDCl_3$), δ (TMS, ppm): 7.40, 7.25, 7.21, 7.04, 6.88, 6.39, 3.28 (8H, $(-NCH_2)_4$), 2.49, 1.86, 1.59, 1.11 (12H, $-(CH_3)_4$). ^{13}C NMR (100 MHz, $CDCl_3$), δ (TMS, ppm): 170.80 (C=O), 149.66, 145.88, 145.39, 144.55, 141.77, 134.76, 132.27, 131.98, 131.05, 130.24, 126.98, 124.85, 121.01, 120.49, 118.91, 110.11, 89.57, 87.73, 43.53 ($-CH_2$), 37.80 ($-(HC{=}C)CH_2$), 33.29 ($-CH_2CH_2CH_2$), 23.19 ($O{=}CCH_2$), 12.07, ($-CH_3$).

Detection of Explosive (PA). A THF solution of **P2** with a concentration of 0.4 μM was prepared. An aliquot (1 mL) of the stock solution was slowly added into 9 mL of water under vigorous shaking by using a Vortex Gene 2 apparatus, resulting in the formation of highly emissive nanoaggregates of **P2** suspended in the aqueous mixture. Aqueous solutions of PA in concentrations of 0.1, 1, and 2 mg/mL were prepared. Different amounts of PA were injected into 3 mL of the nanoaggregate suspensions, and emission intensities of the resultant mixtures were measured.

Preparation of Polyelectrolytes. Water-soluble CPEs $\mathbf{P1}^+$ and $\mathbf{P2}^+$ were prepared by ionizations of **P1** and **P2** using dilute hydrochloric acid solution. The preparation of $\mathbf{P1}^+$ is described below as an example: 50 mg of **P1** was added into 10 mL of 0.3 M hydrochloric acid solution. After stirring at room temperature for about 15 min, the polymer became completely dissolved in the aqueous medium. The mixture was predried by blowing with compressed air. After the water was evaporated, the CPE was further dried under vacuum at room temperature to a constant weight.

CPE/MWNT Hybridization. The procedures for the fabrication of $\mathbf{P1}^+$/MWNT nanohybrid are given below as an example. Into a tube were added 13.2 mg of $\mathbf{P1}^+$, 5.0 mg of MWNTs, and 3 mL of water. After vigorous stirring for 1 h, the mixture was filtered through a cotton filter to remove the unwrapped, insoluble MWNTs. Water was evaporated, and the soluble nanohybrid was dried at 120 °C to a constant weight.

Protein Quantitation. The stock solutions of BSA with concentrations of 0.1 and 1 mg/mL were prepared by dissolving appropriate amounts of the protein in aqueous phosphate buffer. Fluorescence titration was carried out by adding aliquots of BSA solution in the aqueous phosphate buffer to 20 μL of 1 mg/mL solution of $\mathbf{P2}^+$, followed by the addition of a proper amount of the pH 7.0 buffer to acquire a 10 mL solution. The BSA and $\mathbf{P2}^+$ solutions were measured and transferred by 25 μL microsyringes.

Acknowledgment. This work was partially supported by the Hong Kong Research Grants Council (603509, 603008 and HKUST13/CRF/08), The National Science Foundation of China (20974028 and 20634020), and the Ministry of Science & Technology (2009CB623605). B.Z.T. thanks the support from the Cao Guangbiao Foundation of Zhejiang University.

Supporting Information Available: ^1H NMR spectra of **1** and **P1** in DCM-d_2 and DMSO-d_6, ^{13}C NMR spectra of **1** and **P1** in chloroform-*d*, IR spectra of **2** and **P2**, ^1H NMR and ^{13}C NMR spectra of **2** and **P2** in chloroform-*d*, TGA thermograms of **P1** and **P2**, emission spectra of **P2** in toluene, THF and DMF, chemical structure of $\mathbf{2}^+$, emission spectra of $\mathbf{2}^+$ in aqueous phosphate buffer, photographs of $\mathbf{2}^+$ in aqueous buffer, and photographs of **2** and **P2** in THF. This material is available free of charge via the Internet at http://pubs.acs.org.

References and Notes

(1) (a) Hadziioannou, G., van Hutten, P. F., Eds.; *Semiconducting Polymers: Chemistry, Physics and Engineering*, 1st ed.: Wiley-VCH: Weinheim, Germany, 2000. (b) Grimsdale, A. C.; Chan, K. L.; Martin, R. E.; Jokisz, P. G.; Holmes, A. B. *Chem. Rev.* **2009**, *109*, 897. (c) Liu, J. Lam, J. W. Y.; Tang, B. Z. *Chem. Rev.* **2009**, *109*, 5799.

(2) (a) Burroughs, J. H.; Bradley, D. D. C.; Brown, A. B.; Marks, R. N.; Mackay, K.; Friend, R. H.; Burn, P. L.; Holmes, A. B. *Nature* **1990**, *347*, 539. (b) Sirringhaus, H.; Tessler, N.; Friend, R. H. *Science* **1998**, *280*, 1741. (c) Pei, J.; Yu, W.-L.; Huang, W.; Heeger, A. J. *Macromolecules* **2000**, *33*, 2462. (d) Huyal, I. O.; Koldemir, U.; Ozel, T.; Demir, H. V.; Tuncel, D. *J. Mater. Chem.* **2008**, *18*, 3568.

(3) (a) Chen, L.-M.; Hong, Z.; Li, G.; Yang, Y. *Adv. Mater.* **2009**, *21*, 1434. (b) Chen, C.-P.; Chan, S.-H.; Chao, T.-C.; Ting, C.; Ko, B.-T. *J. Am. Chem. Soc.* **2008**, *130*, 12828. (c) Li, Y.; Zou, Y. *Adv. Mater.* **2008**, *20*, 2952.

(4) (a) Katz, H. E.; Bao, Z.; Gilat, S. L. *Acc. Chem. Res.* **2001**, *34*, 359. (b) Li, Y.; Wu, Y.; Ong, B. S. *Macromolecules* **2006**, *39*, 6521.

(5) (a) Davis, W. B.; Svec, W. A.; Ratner, M. A.; Wasielewski, M. R. *Nature* **1998**, *396*, 60. (b) Lipton-Duffin, J. A.; Ivasenko, O.; Perepichka, D. F.; Rosei, F. *Small* **2009**, *5*, 592.

(6) (a) Jager, E. W. H.; Smela, E.; Inganäs, O. *Science* **2000**, *290*, 1540. (b) Holdcroft, S. *Adv. Mater.* **2001**, *13*, 1753.

(7) Smela, E. *Adv. Mater.* **2003**, *15*, 481 and references therein.

(8) McGehee, M. D.; Heeger, A. J. *Adv. Mater.* **2000**, *12*, 1655.

(9) Spangler, C. W. *J. Mater. Chem.* **1999**, *9*, 2013.

(10) Thomas, S. W.III; Joly, G. D.; Swager, T. M. *Chem. Rev.* **2007**, *107*, 1339.

(11) Pei, Q.; Yu, G.; Zhang, C.; Yang, Y.; Heeger, A. J. *Science* **1995**, *269*, 1086.

(12) (a) Shirakawa, H. *Angew. Chem., Int. Ed.* **2001**, *40*, 2575. (b) MacDiarmid, A. G. *Angew. Chem., Int. Ed.* **2001**, *40*, 2581. (c) Heeger, A. J. *Angew. Chem., Int. Ed.* **2001**, *40*, 2591.

(13) (a) Lam, J. W. Y.; Tang, B. Z. *J. Polym. Sci., Part A: Polym. Chem.* **2003**, *41*, 2607. (b) Lam, J. W. Y.; Tang, B. Z. *Acc. Chem. Res.* **2005**, *38*, 745. (c) Masuda, T. *J. Polym. Sci., Part A: Polym. Chem.* **2007**, *45*, 165.

(14) (a) Choi, S. K.; Gal, Y. S.; Jin, S. H.; Kim, H. K. *Chem. Rev.* **2000**, *100*, 1645. (b) Masuda, T.; Tang, B. Z.; Higashimura, T.; Yamaoka, H. *Macromolecules* **1985**, *18*, 2369.

(15) (a) Yashima, E.; Maeda, K.; Furusho, Y. *Acc. Chem. Res.* **2008**, *41*, 1166. (b) Rudick, J. G.; Percec, V. *Macromol. Chem. Phys.* **2008**, *209*, 1760.

(16) (a) Kong, X.; Lam, J. W. Y.; Tang, B. Z. *Macromolecules* **1999**, *32*, 1722. (b) Lam, W. Y.; Dong, Y.; Tang, B. Z. *Macromolecules* **2002**, *35*, 8288. (c) Kwak, G.; Minakuchi, M.; Sakaguchi, T.; Masuda, T.; Fujiki, M. *Chem. Mater.* **2007**, *19*, 3654.

(17) Tabata, M.; Sadahiro, Y.; Nozaki, Y.; Inaba, Y.; Yokota, K. *Macromolecules* **1996**, *29*, 6673.

(18) (a) Tang, B. Z.; Chen, H.; Lam, W. Y.; Wang, M. *Chem. Mater.* **2000**, *12*, 213. (b) Lam, J. W. Y.; Cheuk, K. K. L.; Tang, B. Z. *Polym. Mater. Sci. Eng.* **2003**, *89*, 496.

(19) (a) Buchmeiser, M. R.; Schuler, N.; Kaltenhauser, G.; Ongania, K.-H.; Lagoja, I.; Wurst, K.; Schottenberger, H. *Macromolecules* **1998**, *31*, 3175. (b) Yuan, W. Z.; Mao, Y.; Zhao, H.; Sun, J. Z.; Xu, H. P.; Jin, J. K.; Zheng, Q.; Tang, B. Z. *Macromolecules* **2008**, *41*, 701. (c) Yuan, W. Z.; Sun, J. Z.; Liu, J. Z.; Dong, Y.; Li, Z.; Xu, H. P.; Qin, A. J.; Häussler, M.; Jin, J.; Zheng, Q.; Tang, B. Z. *J. Phys. Chem. B* **2008**, *112*, 8896.

(20) (a) Sanda, F.; Araki, H.; Masuda, T. *Macromolecules* **2004**, *37*, 8510. (b) Morino, K.; Maeda, K.; Yashima, E. *Macromolecules* **2003**, *36*, 1480. (c) Li, B. S.; Kang, S. Z.; Cheuk, K. K. L.; Wan, L.; Ling, L.; Bai, C.; Tang, B. Z. *Langmuir* **2004**, *20*, 7598.

(21) Cheuk, K. K. L.; Lam, J. W. Y.; Li, B. S.; Xie, Y.; Tang, B. Z. *Macromolecules* **2007**, *40*, 2633.

(22) (a) Hua, J. L.; Lam, J. W. Y.; Dong, H. C.; Wu, L. J.; Wong, K. S.; Tang, B. Z. *Polymer* **2006**, *47*, 18. (b) Kwak, G.; Fujiki, M.; Sakaguchi, T.; Masuda, T. *Macromolecules* **2006**, *39*, 319. (c) Yuan, W. Z.; Qin, A.; Lam, J. W. Y.; Sun, J. Z.; Dong, Y.; Häussler, M.; Liu, J.; Xu, H. P.; Zheng, Q.; Tang, B. Z. *Macromolecules* **2007**, *40*, 3159.

(23) (a) Chen, J.; Xie, Z.; Lam, J. W. Y.; Law, C. C. W.; Tang, B. Z. *Macromolecules* **2003**, *36*, 1108. (b) Lam, J. W. Y.; Qin, A.; Dong, Y.; Hong, Y.; Jim, C. K. W.; Liu, J.; Dong, Y.; Kwok, H. S.; Tang, B. Z. *J. Phys. Chem. B* **2008**, *112*, 11227.

(24) Qu, J.; Katsumata, T.; Satoh, M.; Wada, J.; Igarashi, J.; Mizoguchi, K.; Masuda, T. *Chem.—Eur. J.* **2007**, *13*, 7965.

(25) (a) Tang, B. Z.; Xu, H. *Macromolecules* **1999**, *32*, 2569. (b) Tang, B. Z.; Xu, H.; Lam, J. W. Y.; Lee, P. P. S.; Xu, K.; Sun, Q.; Cheuk, K. K. L. *Chem. Mater.* **2000**, *12*, 1446. (c) Zhao, H.; Yuan, W. Z.; Tang, L.; Sun, J. Z.; Xu, H. P.; Qin, A.; Mao, Y.; Jin, J. K.; Tang, B. Z. *Macromolecules* **2008**, *41*, 8566. (d) Yuan, W. Z.; Tang, L.; Zhao, H.; Jin, J. K.; Sun, J. Z.; Qin, A.; Xu, H. P.; Liu, J.; Yang, F.; Zheng, Q.; Chen, E.; Tang, B. Z. *Macromolecules* **2009**, *42*, 52.

(26) (a) Zeng, Q.; Cai, P.; Li, Z.; Qin, J.; Tang, B. Z. *Chem. Commun.* **2008**, *9*, 1094. (b) Zeng, Q.; Lam, J. W. Y.; Jim, C. K. W.; Qin, A.; Qin, J.; Li, Z.; Tang, B. Z. *J. Polym. Sci., Part A: Polym. Chem.* **2008**, *46*, 8070.

(27) Rudick, J. G.; Percec, V. *Acc. Chem. Res.* **2008**, *41*, 1641 and references therein.

(28) (a) Luo, J.; Xie, Z.; Lam, J. W. Y.; Cheng, L.; Chen, H.; Qiu, C.; Kwok, H. S.; Zhan, X.; Liu, Y.; Zhu, D.; Tang, B. Z. *Chem. Commun.* **2001**, 1740. (b) Chen, J.; Law, C. C. W.; Lam, J. W. Y.; Dong, Y.; Lo, S. M. F.; Williams, I. D.; Zhu, D.; Tang, B. Z. *Chem. Mater.* **2003**, *15*, 1535. (c) Zeng, Q.; Li, Z.; Dong, Y.; Di, C.; Qin, A.; Hong, Y.; Ji, L.; Zhu, Z.; Jim, C. K. W.; Yu, G.; Li, Q.; Li, Z.; Liu, Y.; Qin, J.; Tang, B. Z. *Chem. Commun.* **2007**, 70. (d) Li, Z.; Dong, Y.; Mi, B.; Tang, Y.; Häussler, M.; Tong, H.; Dong, Y.; Lam, J. W. Y.; Ren, Y.; Sung, H. H. Y.; Wong, K. S.; Gao, P.; Williams, I. D.; Kwok, H. S.; Tang, B. Z. *J. Phys. Chem. B* **2005**, *109*, 10061.

(29) For reviews, see: (a) Hong, Y.; Lam, J. W. Y.; Tang, B. Z. *Chem. Commun.* **2009**, 4332. (b) Liu, J.; Lam, J. W. Y.; Tang, B. Z. *J. Inorg. Organomet. Polym. Mater.* **2009**, *19*, 249.

(30) (a) Dong, Y.; Lam, J. W. Y.; Qin, A.; Sun, J.; Liu, J.; Li, Z.; Sun, J.; Sung, H. H. Y.; Williams, I. D.; Kwok, H. S.; Tang, B. Z. *Chem. Commun.* **2007**, 3255. (b) Li, Z.; Dong, Y. Q.; Lam, J. W. Y.; Sun, J.; Qin, A.; Häussler, M.; Dong, Y. P.; Sung, H. H. Y.; Williams, I. D.; Kwok, H. S.; Tang, B. Z. *Adv. Funct. Mater.* **2009**, *19*, 905. (c) Zhao, Z.; Wang, Z.; Lu, P.; Chan, C. Y. K.; Liu, D.; Lam, J. W. Y.; Sung, H. H. Y.; Williams, I. D.; Ma, Y.; Tang, B. Z. *Angew. Chem., Int. Ed.* **2009**, *48*, 7608.

(31) Cheng, K. H.; Zhong, Y.; Xie, B. Y.; Dong, Y. Q.; Hong, Y.; Sun, J. Z.; Tang, B. Z.; Wong, K. S. *J. Phys. Chem. C* **2008**, *112*, 17507.

(32) (a) Hong, Y.; Häussler, M.; Lam, J. W. Y.; Li, Z.; Sin, K. K.; Dong, Y.; Tong, H.; Liu, J.; Qin, A.; Renneberg, R.; Tang, B. Z. *Chem.—Eur. J.* **2008**, *14*, 6428. (b) Dong, Y.; Lam, J. W.Y.; Qin, A.; Li, Z.; Liu, J.; Sun, J.; Dong, Y.; Tang, B. Z. *Chem. Phys. Lett.* **2007**, *446*, 124. (c) Tong, H.; Hong, Y.; Dong, Y.; Häussler, M.; Lam, J. W. Y.; Li, Z.; Guo, Z.; Guo, Z.; Tang, B. Z. *Chem. Commun.* **2006**, 3705. (d) Wang, M.; Zhang, D.; Zhang, G.; Tang, Y.; Wang, S.; Zhu, D. *Anal. Chem.* **2008**, *80*, 6443.

(33) Yu, Y.; Hong, Y.; Feng, C.; Liu, J.; Lam, J. W. Y.; Faisal, M.; Ng, K. M.; Luo, K. Q.; Tang, B. Z. *Sci. China, Ser. B* **2009**, *52*, 15.

(34) (a) Dwight, S. J.; Gaylord, B. S.; Hong, J. W.; Bazan, G. C. *J. Am. Chem. Soc.* **2004**, *126*, 16850. (b) Liu, B.; Bazan, G. C. *Chem. Mater.* **2004**, *16*, 4467. (c) Achyuthan, K. E.; Bergstedt, T. S.; Chen, L.; Jones, R. M.; Kumaraswamy, S.; Kushon, S. A.; Ley, K. D.; Lu, L.; McBranch, D.; Mukundan, H.; Rininsland, F.; Shi, X.; Xia, W.; Whitten, D. G. *J. Mater. Chem.* **2005**, *15*, 2648. (d) Hoven, C. V.; Garcia, A.; Bazan, G. C.; Nguyen, T.-Q. *Adv. Mater.* **2008**, *20*, 3793. (e) Ho, H. A.; Najari, A.; Leclerc, M. *Acc. Chem. Res.* **2008**, *41*, 168. (f) Jiang, H.; Taranekar, P.; Reynolds, J. R.; Schanze, K. S. *Angew. Chem., Int. Ed.* **2009**, *48*, 4300.

(35) Georgakilas, V.; Gournis, D.; Tzitzios, V.; Pasquato, L.; Guldi, D. M.; Prato, M. *J. Mater. Chem.* **2007**, *17*, 2679 and references therein.

(36) (a) Pinto, M. R.; Schanze, K. S. *Proc. Natl. Acad. Sci. U.S.A.* **2004**, *101*, 7505. (b) Pu, K.-Y.; Liu, B. *Adv. Funct. Mater.* **2009**, *19*, 277. (c) Pu, K.-Y.; Liu, B. *Adv. Funct. Mater.* **2009**, *19*, 1371.

(37) Saeed, I.; Shiotsuki, M.; Masuda, T. *Macromolecules* **2006**, *39*, 5347.

(38) Kishimoto, Y.; Itou, M.; Miyatake, T.; Ikariya, T.; Noyori, R. *Macromolecules* **1995**, *28*, 6662.

(39) Hu, R.; Lager, E.; Aguilar-Aguilar, A.; Liu, J.; Lam, J. W. Y.; Sung, H. H.-Y.; Williams, I. D.; Zhong, Y.; Wong, K. S.; Peña-Cabrera, E.; Tang, B. Z. *J. Phys. Chem. C* **2009**, *113*, 15845.

(40) (a) Wong, K. S.; Lee, C. W.; Tang, B. Z. *Synth. Met.* **1999**, *101*, 505. (b) Lee, C. W.; Wong, K. S.; Lam, W. Y.; Tang, B. Z. *Chem. Phys. Lett.* **1999**, *307*, 67.

(41) (a) Huang, Y. M.; Lam, J. W. Y.; Cheuk, K. K. L.; Ge, W.; Tang, B. Z. *Macromolecules* **1999**, *32*, 5976. (b) Yuan, W. Z.; Lam, J. W. Y.; Shen, X. Y.; Sun, J. Z.; Mahtab, M.; Zheng, Q.; Tang, B. Z. *Macromolecules* **2009**, *42*, 2523.

(42) Sohn, H.; Sailor, M. J.; Magde, D.; Trogler, W. C. *J. Am. Chem. Soc.* **2003**, *125*, 3821.

(43) (a) Cheuk, K. K. L.; Lam, J. W. Y.; Lai, L. M.; Dong, Y. P.; Tang, B. Z. *Macromolecules* **2003**, *36*, 9752. (b) Cheuk, K. K. L.; Li, B. S.; Lam, J. W. Y.; Xie, Y.; Tang, B. Z. *Macromolecules* **2008**, *41*, 5997. (c) Cheuk, K. K. L.; Lam, J. W. Y.; Chen, J.; Lai, L. M.; Tang, B. Z. *Macromolecules* **2003**, *36*, 5947. (d) Lai, L. M.; Lam, J. W. Y.; Qin, A.; Dong, Y.; Tang, B. Z. *J. Phys. Chem. B* **2006**, *110*, 11128. (e) Li, B.; Cheuk, K. K. L.; Salhi, F.; Lam, J. W. Y.; Cha, J. A. K.; Xiao, X.; Bai, C.; Tang, B. Z. *Nano Lett.* **2001**, *1*, 323.

(44) Schrock, R. R.; Osborn, J. A. *Inorg. Chem.* **1970**, *9*, 2339.

(45) Hirao, K.; Ishii, Y.; Terao, T.; Kishimoto, Y.; Miyatake, T.; Ikariya, T.; Noyori, R. *Macromolecules* **1998**, *31*, 3405.